Thermal variations of iodine nanostructures inside the channels of $AlPO_4$-5 zeolite single crystals

J. T. Ye,[1,2,*] Y. Iwasa,[2] and Z. K. Tang[1]

[1]*Department of Physics and Institute of Nano Science and Technology, Hong Kong University of Science and Technology, Clear Water Bay, Kowloon, Hong Kong, China*

[2]*Quantum-Phase Electronics Center and Department of Applied Physics, The University of Tokyo, 7-3-1 Hongo, Bunkyo-ku, Tokyo 113-8656, Japan*

(Received 6 September 2010; revised manuscript received 7 February 2011; published 25 May 2011)

The structural changes of ordered hexagonal arrays of iodine nanostructures enclosed inside one-dimensional channels of aluminophosphate zeolites are studied. These isolated nanochains undergo structural transformations between linked chains and separated molecules, as shown by tracing the temperature variations of their distinctive Raman features when these nanostructures are heated thermally to the transition temperature of ~70 °C. The reversibility of this transition is improved by replacing the conventional thermal heating with localized heating using a focused laser beam, which reduced the diffusion along the channels. In addition, the optically identified transition is consistently confirmed by thermal characterization using differential scanning calorimetric and thermal gravimetric analyses.

DOI: 10.1103/PhysRevB.83.193409 PACS number(s): 81.07.Gf, 82.75.Vx, 78.30.Ly, 65.60.+a

Confining nanostructures or molecules inside a microporous framework creates a unique composite system with inherent interactions between the material and pores, which play a role in the thermal properties of enclosed materials.[1,2] Scientifically, the confined geometry significantly changes the structural and dynamic properties of these nanostructures from the bulk or from the nanostructures in their freestanding states.[1–4] Technically, the phase properties showing structural transformation of enclosed nanostructures or molecules are closely related to understanding the functional performance of porous materials as media for storage,[5–8] microsieves for separation,[9,10] or hosts for catalysis.[11] Experimental studies on the thermal properties of these systems, especially for the one-dimensional (1D) case, have been limited by the availability of well-defined 1D systems despite the above scientific and technical importance. Recently, well-aligned nanostructures formed inside the framework of porous 1D channels of zeolite single crystals provide a qualified platform to probe the structural transformation properties in the 1D confined regime.[12,13]

In this Brief Report, we report the structural transformation of iodine nanostructures formed inside the channels of aluminophosphate zeolite single crystals ($AlPO_4$-5, IUPAC code: AFI),[14] which provides an excellent example for exploring novel phase properties within 1D systems. The interchain interactions between these structures are negligible because all the nanostructures are isolated and enclosed within separated channels.[15] Based on our previous optical study, three different iodine structures were found as linked nanochains; $(I_2)_n$ and $(I_n)^-$, the two major phases coexisting with one minority phase of separated I_2 molecules.[13] These iodine nanostructures were introduced inside the AFI channels [iodine@AFI, as shown in the inset of Fig. 1(b)] through a physical vapor transport method, as reported in previous studies.[13] We sealed the dehydrated AFI single crystals (with the tripropylamine organic growth template removed by calcination[16]) with pure iodine (BDH 99%) inside Pyrex tubes and then heated the crystals from 200 to 300 °C. The structural transformation of as-grown iodine@AFI crystals was characterized by means of *in situ* Raman spectroscopy (T64000, Jobin Yvon) on single crystals under thermal heating. We also controlled the structural transformation by localized thermal heating using a focused laser beam with elevated power. Simultaneously, Raman-scattering spectra with the same excitation were measured within a localized area (<1 μm^2, using a 100× microscope objective at 514.5 nm) defined by the focus. Furthermore, we confirmed the structural transformation by differential scanning calorimetry (DSC) and thermal gravimetry (TG) (449A, Netsch) using 10 mg iodine@AFI.

Using micro-Raman spectroscopy, information on the structural variations of iodine chains near their structural transformation temperature can be clearly distinguished by the characteristic Raman modes from different iodine species. Figure 1 shows the temperature evolution of the Raman spectra. Close to room temperature (at ~30 °C), the Raman spectra show typical scattering features at 110 and 168 cm^{-1} originating from the $(I_3)^-$ and $(I_2)_n$ iodine nanostructures, respectively. In addition, we observed trace Raman scattering at 209 cm^{-1} (from iodine molecules I_2). It is worth noting that the Raman intensities from iodine nanostructures are much stronger than those from iodine molecules, indicating that the pristine iodine@AFI samples are dominated by the nanostructure phases. As shown in Fig. 1(a), the temperature dependences of the Raman modes exhibit diminishing intensities of the scattering from the two modes of iodine nanostructures upon heating from 30 to 125 °C, leaving only blurred features at 125 °C. The evolution of the Raman mode from iodine molecules at 209 cm^{-1} is opposite to those of the nanostructures and dominates the Raman spectra at 125 °C.

We attribute this contrasting behavior in the temperature evolution of Raman modes to the phase change between nanostructures and molecules during the transition process. As shown by the Raman scattering in Fig. 1(a), the iodine nanostructures are the main phase for temperatures lower than the transition and dissociate into iodine molecules when the system reaches the transition temperature, as indicated by the decrease (168 cm^{-1}) and increase (209 cm^{-1}) of Raman scattering from the phases of the iodine chains and molecules,

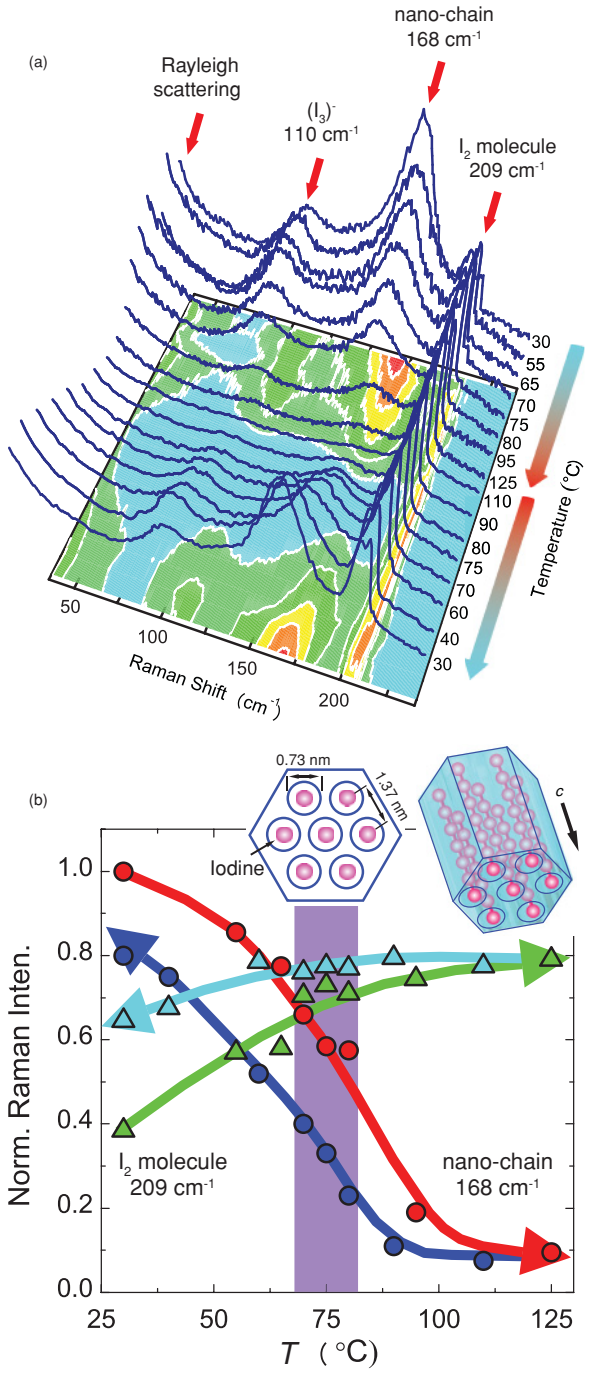

FIG. 1. (Color online) Temperature dependence of Raman spectra of iodine chains formed inside AFI zeolites. (a) Raman spectra were measured in the temperature ranges 30–125 °C and 110–30 °C (as indicated by the arrows) for increasing and decreasing T, respectively. Raman scattering is identified for different iodine structures, including $(I_3)^-$ and nanochains, as well as residues of I_2 molecules. The bottom plane shows the intensity map of Raman scattering with colored contours corresponding to the high (red) and low (blue) intensities. (b) Temperature dependence of integrated Raman scattering from iodine nanochains (168 cm^{-1}) and molecules (209 cm^{-1}). The solid lines provide guides for the eyes, with the arrows showing the directions of the scanning temperature. Quick changes in the intensities are found in the range 70–80 °C (purple shading). The inset shows schematic representations of the structure of AFI single crystal and the enclosed iodine chains along the c axis.

respectively. The structural transformation is suggested not only by the change in the intensity of the Raman modes but also by the change in the vibration energies. With the increase of temperature, the Raman signal at 168 cm^{-1} is upshifted and does not follow the ordinary temperature dependence of Raman modes. Higher temperatures usually soften chemical bonds, causing a downshift of the Raman modes. The observed anomalous frequency upshift can be attributed to the strengthening of bonds between individual iodines in the chains when they become shorter by dissociation.[17] When the temperature decreases from 110 back to 30 °C, the Raman spectra reinstate the features dominated by iodine nanostructures. Although reversible, comparisons between the spectra before and after the transition show a weaker intensity of Raman scattering from the iodine nanostructures and an increase in the iodine molecular modes.

Figure 1(b) shows the temperature dependence of the integrated intensities of Raman scattering from nanochains (168 cm^{-1}) and molecules (209 cm^{-1}). The intensities of these modes are normalized by the temperature variation of the phonon population described by the Bose-Einstein distribution, $n(\omega) = 1/[\exp(\hbar\omega/k_B T) - 1]$, which removes the thermally related variations of the phonon population at the different temperature T. If we neglect the change in the scattering cross section of the same phase with temperature, the relative variations of the Raman intensities are mainly related to changes in the populations of different phases. In the low-temperature range, the change in the relative intensity of Raman spectra from the nanostructures is small, implying only weak distortions in these nanochains. Upon reaching the transition temperature, there is a significant interchange in the Raman intensities of the chain and molecule modes. A quick change in the integrated intensity is identified at temperatures around 70–80 °C, corresponding to the structural transformation temperature.

The temperature dependence of Raman scattering describes the structural transformation in a scenario where iodine molecules are dissociated from the nanochains, changing the length of the nanostructures under heating. However, the Raman intensities before and after one heating and cooling cycle are not identical, indicating that the nanostructures of iodine are not fully recovered after one phase of the transition cycle. One possible reason for this incomplete reversibility is the diffusion of iodine molecules along the free space inside zeolite frameworks after their dissociation from the nanochains; the molecules that diffuse away cannot be fully reassociated with the nanostructures, even when the temperature decreases. Such a scenario is consistent with the temperature dependence of Raman modes of iodine molecules (209 cm^{-1}), for which the change of intensity near the structural transformation temperature is less pronounced compared with that from the iodine chains. On the other hand, other effects could also contribute to the change of intensity of Raman scattering. For instance, the resonant properties of the iodine chains could be changed since its interaction with the channel walls is also affected by thermal heating. Clarification of other contributions need separate studies.

To restrain the diffusion of iodine molecules along the AFI channels, we heated the iodine@AFI crystal locally within an area of less than 1 μm^2 by focusing a laser beam with a

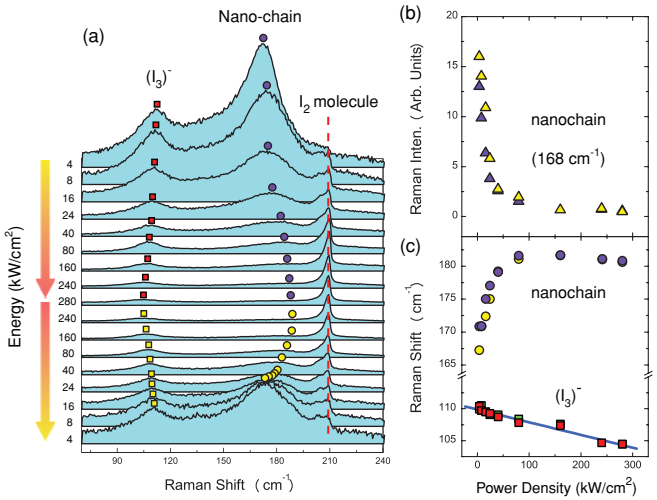

FIG. 2. (Color online) Variation in Raman modes as a function of the incident laser power density. (a) The variation of Raman modes at 110 and 168 cm^{-1} under laser power densities ranging from 4×10^3 to 2.80×10^5 W/cm^2. The dots and squares denote the positions of the Raman modes of $(I_3)^-$ and nanochains, respectively. (b) Variation of integrated Raman scattering from $(I_3)^-$ and nanochains at different incident laser densities. (c) Spectral shifts of Raman modes at 110 and 168 cm^{-1} at different incident laser densities. The solid line is a linear fit of the shift of Raman modes of $(I_3)^-$.

100× microscope objective. Figure 2(a) shows the variation of Raman spectra with the incident laser power. The intensities of the Raman spectra are normalized to the incident photon flux as the laser power was changed from 1 to 70 mW, corresponding to excitation power densities from 4 to 280 kW/cm^2 on the surface of the crystal. At the lowest excitation power, the two strong Raman signals at 110 and 168 cm^{-1} indicate the dominance of $(I_3)^-$ and nanochains. With the increase of the incident laser power, the Raman signal of the $(I_3)^-$ chain slightly shifts to a lower frequency, from 110 to 104 cm^{-1}. As shown in Fig. 2(c), the shift can be fitted linearly with respect to the excitation power. Because the excitation laser wavelength (514.5 nm) is within the optical absorption of the $(I_3)^-$ structure, the downshift of the $(I_3)^-$ mode (110 cm^{-1}) could be attributed to the softening of the phonon mode caused by an increasing temperature. The linear dependence of this Raman mode on the laser power also implies the same linear dependence of temperature on the incident laser power. When the incident laser power is reduced, the Raman frequency of the $(I_3)^-$ mode shifts upward reversibly. For iodine chains, in contrast, the Raman mode (168 cm^{-1}) shifts to a higher frequency, accompanied by a continuous decrease in intensity. Simultaneously, the molecular mode (209 cm^{-1}) increases significantly with the increase in the incident laser power, which is consistent with that observed using thermal heating. The continuous intensity variations and spectral shifts in these two Raman modes also suggest a picture of a structural transformation involving the consecutive dissociation of iodine molecules when long chains of nanostructures reduce to shorter ones and, eventually, to molecules; that is, the length of iodine chains can be controlled using simple localized laser irradiation. As shown in Figs. 2(b) and 2(c), the intensity variation and frequency shift of the Raman modes show higher reversibility in a cycle of power variation of laser excitation. We can possibly attribute this higher reversibility to lesser diffusion of the iodine molecules due to localized heating.

In a separate analysis, the transition observed optically by Raman scattering was further studied by measuring the thermal properties of these iodine nanostructures. Figure 3 shows the DSC/TG analysis of the iodine@AFI samples in the temperature range 30–600 °C (heating rate: 5 °C/min). An endothermic peak at 71 °C for the structural transformation of the enclosed iodine nanostructures is observed in accordance with that determined by Raman scattering, as shown in Figs. 1(a) and 2(a). Compared with bulk iodine single crystals, the structural transformation of these nanostructures appeared at slightly lower temperatures, which is consistent with the confined geometry.[1] From the TG curve, typical dehydration due to the desorption of water (enclosed water molecules inside the channel) at around 100 °C is not noticeable due to the moisture-free handling of the sample.[13] Upon increasing the temperature above 200 °C, the weight of the sample begins to decrease significantly due to the release of volatile iodine molecules from the channels. The two endothermic DSC features at 360 and 470 °C correspond to the weight changes that occur when the iodine molecules are desorbed from the channels. The mass loss is not saturated, even at temperatures higher than 530 °C, due to the slow desorption of enclosed iodine. A nearly full release of enclosed iodine (>90%) is only achieved by calcinations at 600 °C for more than six hours.

As shown in Fig. 3, the total weight loss in the TG analysis is 9.8%, which indicates a low iodine concentration even at the saturated doping stage. As shown in the inset of Fig. 1(b), the structure of the aluminophosphate zeolite single crystal has 1D parallel and hexagonal-packed channels with inner diameters and neighboring-channel distances of 0.73 and 1.37 nm, respectively. Assuming all $AlPO_4$-5 channels are completely

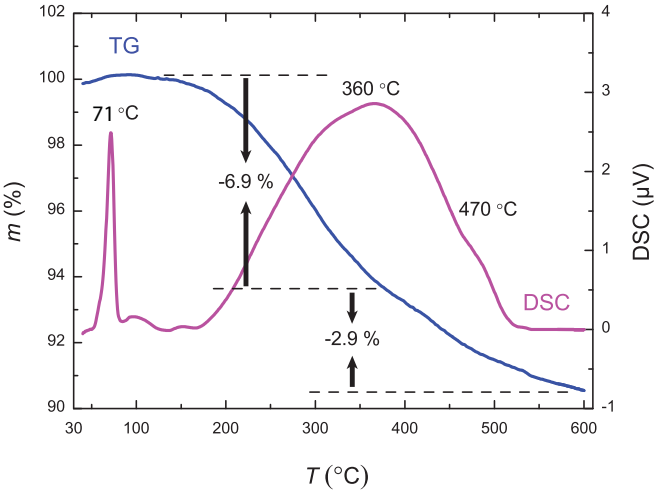

FIG. 3. (Color online) DSC and TG analyses of iodine@AFI. Three DSC features are found at 71, 360, and 470 °C corresponding to the structural transformation (71 °C) and desorption of iodine (360 and 470 °C). The corresponding changes in TG for the iodine desorption process show the weight changes of −2.9 and −6.9% at temperatures of 360 and 470 °C, respectively.

filled with iodine molecules with the molecules aligning into single lines with 0.68 nm van de Waals separation,[18] the weight percentage of iodine versus the composite system is 35.6%. The weight loss of the saturation-loaded sample indicates that approximately 27% of the space is occupied by iodine. As a result, iodine chains are formed only locally inside the channels. The nonuniform density distribution of the iodine is consistent with the Raman spectroscopy study, in which conventional thermal heating shows a lower reversibility than localized heating by a focused laser beam.

In summary, the structural transformation of enclosed iodine structures are observed by Raman scattering and confirmed by thermal analysis. Localized laser heating improves the reversibility of this transition. Understanding the rich phase properties of confined materials provides important information for controlling their states inside such frameworks, which is crucial for improving the performance of applications using porous materials as carrying media.[5–11]

The authors are grateful to P. Sheng, C. T. Chan, and N. Nagasawa for stimulating discussions. This research was supported by Hong Kong CERGC Grant No. 605003, Hong Kong RGC Grant No. DAG05/06.SC33, and RGC Central Allocation Grant No. CA04/05.SC02.

*yejianting@ap.t.u-tokyo.ac.jp

[1]L. D. Gelb, K. E. Gubbins, R. Radhakrishnan, and M. Sliwinska-Bartkowiak, Rep. Prog. Phys. **62**, 1573 (1999).

[2]H. K. Christenson, J. Phys.: Condens. Matter **13**, R95 (2001).

[3]C. Alba-Simionesco, B. Coasne, G. Dosseh, G. Dudziak, K. E. Gubbins, R. Radhakrishnan, and M. Sliwinska-Bartkowiak, J. Phys.: Condens. Matter **18**, R15 (2006).

[4]L. Alvarez, J. L. Bantignies, R. Le Parc, R. Aznar, J. L. Sauvajol, A. Merlen, D. Machon, and A. San Miguel, Phys. Rev. B **82**, 205403 (2010).

[5]R. Matsuda *et al*., Nature (London) **436**, 238 (2005).

[6]X. B. Zhao, B. Xiao, A. J. Fletcher, K. M. Thomas, D. Bradshaw, and M. J. Rosseinsky, Science **306**, 1012 (2004).

[7]M. Eddaoudi, J. Kim, N. Rosi, D. Vodak, J. Wachter, M. O'Keeffe, and O. M. Yaghi, Science **295**, 469 (2002).

[8]H. K. Chae, D. Y. Siberio-Perez, J. Kim, Y.-B. Go, M. Eddaoudi, A. J. Matzger, M. O'Keeffe, and O. M. Yaghi, Nature (London) **427**, 523 (2004).

[9]M. E. Kosal, J. H. Chou, S. R. Wilson, and K. S. Suslick, Nat. Mater. **1**, 118 (2002).

[10]D. Bradshaw, T. J. Prior, E. J. Cussen, J. B. Claridge, and M. J. Rosseinsky, J. Am. Chem. Soc. **126**, 6106 (2004).

[11]J. S. Seo, D. Whang, H. Lee, S. I. Jun, J. Oh, Y. J. Jeon, and K. Kim, Nature (London) **404**, 982 (2000).

[12]V. V. Poborchii, A. V. Kolobov, J. Caro, V. V. Zhuravlev, and K. Tanaka, Phys. Rev. Lett. **82**, 1955 (1999).

[13]J. T. Ye, Z. K. Tang, and G. G. Siu, Appl. Phys. Lett. **88**, 073114 (2006).

[14]The AFI single crystal has one-dimensional parallel and hexagonal-packed channels with 0.73 nm inner diameter and 1.317 nm neighboring-channel distance.

[15]H. D. Sun, Z. K. Tang, W. M. Zhao, and G. K. L. Wong, Appl. Phys. Lett. **71**, 2457 (1997).

[16]Z. K. Tang, Michael M. T. Loy, Jiesheng Chen, and Ruren Xu, Appl. Phys. Lett. **70**, 34 (1997).

[17]E. Mulazzi, I. Pollini, L. Piseri, and R. Tubino, Phys. Rev. B **24**, 3555 (1981).

[18]T. Hertzsch, F. Budde, E. Weber, and J. Hulliger, Angew. Chem., Int. Ed. **41**, 2282 (2002).